Solid State Ionics 193 (2011) 52–59

Contents lists available at ScienceDirect

Solid State Ionics

journal homepage: www.elsevier.com/locate/ssi

Microstructure-property relations in composite yttria-substituted zirconia solid electrolytes

C.M. Fernandes, A. Castela, F.M. Figueiredo *, J.R. Frade

Dep. Ceramics and Glass Engineering, CICECO, University of Aveiro, 3810-193 Aveiro, Portugal

ARTICLE INFO

Article history:
Received 30 September 2010
Received in revised form 1 February 2011
Accepted 17 February 2011
Available online 17 May 2011

Keywords:
ZrO_2
Composites
Microstructure
Grain boundary
Ionic conductivity
Mechanical properties

ABSTRACT

A study of composite 8 mol% yttria stabilized zirconia (8YSZ) and 3 mol% yttria tetragonal zirconia polycrystal (3YTZP) solid electrolytes sintered under isothermal and two-step sintering cycles is reported. The nominal phase composition is retained for composites with up to 25 wt.% 3YTZP. These composites show a combination of beneficial effects with respect to pure 8YSZ, including slight improvement in sinterability, gains in bulk and grain boundary conductivity and also enhanced fracture toughness. Impedance spectroscopy revealed an enhancement of the specific grain boundary conductivity for samples with finer grain sizes, attained by increasing the fraction of 3YTZP or by hindering grain growth under two-step sintering cycles. This effect is rationalized in terms of a decrease of the grain boundary space-charge potential. The conductivity gains decrease with increasing temperature, but even at 700 °C the total ionic conductivity of ceramics with 25 wt.% 3YTZP is still higher than that of pure 8YSZ, whereas at 900 °C there is a performance loss of less than 10%. The improved mechanical and electrical performance in the intermediate temperature range represents an important advantage of the heterostructured electrolytes for low/intermediate temperature SOFC operation.

1. Introduction

Minor additions of a second phase have been used to enhance the properties of zirconia-based solid electrolytes, with emphasis on the beneficial scavenging effect on grain boundary ionic conductivity and enhanced mechanical properties such as fracture toughness [1–4]. An alternative approach was reported recently, based on mixtures of tetragonal and cubic yttria-substituted zirconia mixtures [5], or core–shell approaches obtained from tetragonal zirconia polycrystal powders coated with a scandia [6] or yttria gel [7]. These authors reported significant enhancement of strength and fracture toughness, and also increased conductivity for selected ranges of the tetragonal: cubic phases ratio. There was also clear evidence of the coexistence of tetragonal and cubic zirconia phases in those ceramic samples.

Recent findings indicate that long-term exposure to typical solid oxide fuel cell (SOFC) operating conditions is likely to cause partial precipitation of the tetragonal phase from the pristine cubic phase [8,9]. Indeed, relative conductivity changes on long term aging are greater with decreasing contents of yttria [9], i.e., on approaching the single phase boundary of the phase diagram [10]. Others ascribed aging to increasing interactions between charge carriers (oxide ion vacancies) and the trivalent additive [11]. Indeed, tetragonal zirconias are more likely to undergo degradation by partial transformation to monoclinic, especially in wet environments or even by mechanical stimulation [12]. To some extent, there is also evidence of slight long-term changes of cubic zirconia in boiling water [13]. The corresponding conductivity changes were interpreted by a space-charge model [13,14], based on the assumption of interactions between hydroxyl ions and oxygen vacancies, and depletion of vacancies at grain boundaries.

Two-phase materials are expected for the binary oxide system ZrO_2–Y_2O_3 with moderate fractions of yttria [10], yielding partially stabilized zirconias with superior mechanical properties when the fraction of tetragonal phase is sufficiently high and well dispersed in the cubic matrix [15]. This is another reason for considering composite cubic-tetragonal zirconia solid electrolytes, as demonstrated for samples prepared from powder mixtures containing 35 wt.% of 3 mol% yttria zirconia polycrystals (3YTZP) in 8 mol% yttria-stabilized zirconia (8YSZ) [5]. The present work extends the analysis to compositions ranging from 100% 8YSZ, to 100% 3YTZP, and examines the microstructural effects on bulk and grain boundary properties in detail. This further includes samples obtained by two-step sintering schedules that display considerably smaller grains, while minimizing re-mixing of the 3YTZP and 8YSZ phases.

2. Experimental procedures

Mixtures of commercial powders of ZrO_2 with 3 mol% Y_2O_3 and 8 mol% Y_2O_3 (Tosoh Co.) were used to prepare heterogeneous solid electrolytes with 0, 15, 25, 35, 50, 75 and 100 wt.% of 3YTZP, hereafter

---

* Corresponding author. Tel.: +351 234 401 464; fax: +351 234 425 300.
E-mail address: lebre@ua.pt (F.M. Figueiredo).

0167-2738/$ – see front matter © 2011 Elsevier B.V. All rights reserved.
doi:10.1016/j.ssi.2011.02.017

referred to as 8YSZ, 3YTZP15, 3YTZP25, 3YTZP35, 3YTZP50, 3YTZP75 and 3YTZP. The specific surface area (S) of starting powders was 15.4 $m^2\ g^{-1}$ for 3YTZP and 11.8 $m^2\ g^{-1}$ for 8YSZ, as measured from nitrogen adsorption Brunauer–Emmett–Teller isotherms (BET). Average particle diameters of $D \approx 64$ nm for 3YTZP and $D \approx 84$ nm for 8YSZ were estimated assuming the relation $D \approx 6/(S\rho)$ for spherical particles, where ρ is the density. These values were confirmed by transmission electron microscopy (TEM) in a Hitachi 9000 microscope. The starting powders in the required proportions were thoroughly dispersed with ethanol, uniaxially pressed with disk-shape at 50 MPa and then isostatically pressed at 200 MPa. A LINSEIS dilatometer was used to study the shrinkage behavior of powder compacts on heating at 10 °C/min in order to select suitable temperatures for isothermal sintering at (1400 °C for 4h) 1400 °C for 4 h, or an alternative 2-step sintering cycle (TSS). In this case, the temperature was raised at 10 °C min^{-1} up to 1320 °C, then cooled at 10 °C min^{-1}, and isothermally treated for 12 h at 1270 °C, according to a previous detailed study [16]. The complete list of prepared samples, including the sintering conditions and sample notation is shown in Table 1.

The density of sintered disks was determined from the weight and volume of the pellets and expressed as a fraction of the theoretical density (relative density—RD). Scanning electron microscopy (SEM) and energy dispersive spectroscopy (EDS) were used for microstructural characterization and to confirm composition gradients in polished and thermally etched ceramics, using a Hitachi SU-70 microscope with a Bruker Quantax 400 spectrometer. The equivalent grain diameter (G) of the ceramics was estimated by $G = 2(A_g/\pi)^{1/2}$, where A_g is the grain area measured on SEM micrographs of polished surfaces using Image J (v. 1.43u, Wayne Rasband, National Institute of Health. USA). The co-existence of tetragonal and cubic phases was confirmed by X-ray diffraction on a Rigaku diffractometer using CuKα radiation (step of $2\theta = 0.05°$ with an acquisition time of 25 or 50 s per point). The Vickers hardness of the ceramics was measured with a micro hardness tester Shimadzu type M, by application of a load of 98 N for 15 s. The fracture toughness (K_{IC}) was assessed on a Zwick/Roell ZHU indenter by measuring the crack length caused by indentation with a load of 294 N, applied for 15 s, and using the relevant solution for Palmqvist cracks [17]:

$$K_{Ic} = 0.00905\, HV^{3/5} E^{2/5} dc^{-1/2} \tag{1}$$

where E is the Young's modulus, taken as 210 GPa, d is the average diagonal length produced by the indentation and c is the average length of the Palmqvist cracks. Impedance spectroscopy (20 Hz–1 MHz) was used to characterize the samples in the temperature range 250–1000 °C, with porous Pt electrodes obtained with commercial paste. Those data were obtained in air with a Hewlett Packard 4984a LCR meter. The impedance contributions ascribed to grain boundaries and (bulk) grain interiors were obtained after deconvolution of impedance spectra by fitting to conventional equivalent circuits using Z-View (version 2.6b, 1990–2002, Scribner Associates).

Table 1
Composition, notation, sintering schedule and relative density of 3YTZP–8YSZ composites. The suffix TSS refers to the two-step sintering cycles. Heating and cooling rates were fixed at ± 10 °C/min in all cases.

Wt.% 3YTZP	Notation	Sintering conditions	*RD* (%)
0	8YSZ	1400 °C, 4 h	100
15	3YTZP15	1400 °C, 4 h	96
25	3YTZP25	1400 °C, 4 h	100
25	3YTZP25TSS	1320 °C 1270 °C, 12 h	95
35	3YTZP35	1400 °C, 4 h	100
35	3YTZP35TSS	1320 °C 1270 °C, 12 h	99
50	3YTZP50	1400 °C, 4 h	99
50	3YTZP50TSS	1320 °C 1270 °C, 12 h	94
75	3YTZP75	1400 °C, 4 h	100
100	3YTZP	1400 °C, 4 h	100

3. Results and discussion

3.1. Sintering and mechanical properties of ceramics

The kinetics of sintering may be described by a generic Herring equation:

$$\frac{d\rho}{dt} = \frac{K(T).F(\rho_o,\rho)\rho}{TG^n} \tag{2}$$

which expresses the dependence of the density (ρ) on time (t), temperature (T) and grain size (G). The exponent n depends on the sintering mechanism, with a typical value $n = 4$ for grain boundary diffusion. The geometric factor $F(\rho_0, \rho)$ varies with the initial green packing density (ρ_0) and also decreases with increasing density. The temperature dependence may be described by an Arrhenius-type equation of the kinetic constant $K(T) = K_o \exp(-E_a/RT)$, where K_o is a pre-exponential factor and E_a is the activation energy. By further considering the shrinkage on heating at constant rate ($\beta = dT/dt$), the time-dependent Eq. (2) is transformed to the corresponding temperature dependence as follows:

$$ln\left\{\frac{d\ ln(\rho)}{d\ ln(T)}\right\} = -\ ln(\beta) +\ ln(K_o) - \frac{E_a}{RT} +\ ln[F(\rho_o,\rho)] - n\ ln(G). \tag{3}$$

This is the basis for representation of the shrinkage experiments shown in Fig. 1 for 3YTZP, 8YSZ and selected composite powder compacts. It can be seen that the shrinkage rate departs from the expected Arrhenius dependence and reaches a peak at temperatures slightly below 1300 °C for 3YTZP or above 1300 °C for the remaining samples. Moreover, the decay of the densification rate is steeper at higher temperatures, probably and mainly due to the thermal activation of grain growth, which may explain the negative thermal activation above the shrinkage peak. Note also that the decay in the high temperature range is more pronounced for the compositions with prevailing 8YSZ than for compositions with high 3YTZP content, most probably because the activation energy for grain growth is

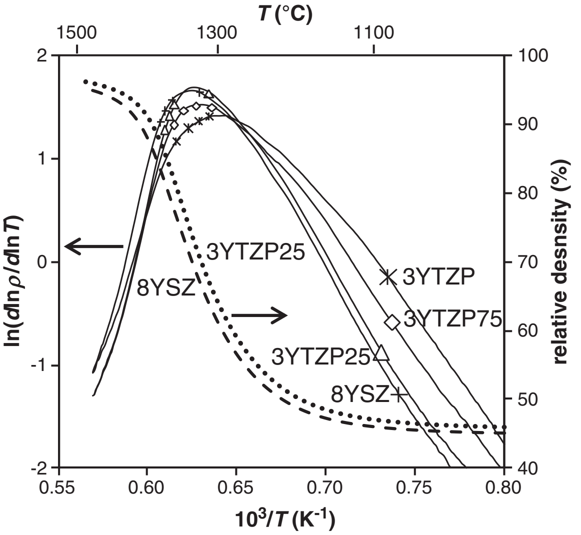

Fig. 1. Dilatometry of representative samples showing effects of additions of 3YTZP to 8YSZ on the sinterability.